STEM CELLS®

TISSUE-SPECIFIC STEM CELLS

PBX1: A Novel Stage-Specific Regulator of Adipocyte Development

MIGUEL C. MONTEIRO,[a,b] MRINMOY SANYAL,[c] MICHAEL L. CLEARY,[d] CORALIE SENGENÈS,[e] ANNE BOULOUMÉ,[e] CHRISTIAN DANI,[a,b] NATHALIE BILLON[a,b]

[a]CNRS, IBDC, Nice, France; [b]Université de Nice-Sophia Antipolis, IBDC, Nice, France; [c]Department of Pediatrics, [d]Department of Pathology, Stanford University School of Medicine, Stanford, California, USA; [e]INSERM U1048, Université Toulouse III Paul Sabatier, Institut des maladies métaboliques et cardiovasculaires de Rangueil, IFR 150, Toulouse, France

Key Words. Pbx1 • Adipogenesis • Embryonic stem cells • Adipose stem cells

ABSTRACT

Although adipocyte terminal differentiation has been extensively studied, the early steps of adipocyte development and the embryonic origin of this lineage remain largely unknown. Here we describe a novel role for the pre-B-cell leukemia transcription factor one (PBX1) in adipocyte development using both mouse embryonic stem cells (mESCs) and human multipotent adipose-derived stem (hMADS) cells. We show that *Pbx1*$^{-/-}$ mESCs are unable to generate adipocytes, despite normal expression of neuroectoderm and neural crest (NC) markers. Early adipocyte lineage markers are not induced in *Pbx1*$^{-/-}$ mESCs, suggesting that *Pbx1* controls the generation and/or the maintenance of adipocyte progenitors (APs) from the NC. We further characterize the function of PBX1 in postnatal adipogenesis and show that silencing of *PBX1* expression in hMADS cells reduces their proliferation by preventing their entry in the S phase of the cell cycle. Furthermore, it promotes differentiation of hMADS cells into adipocytes and partially substitutes for glucocorticoids and rosiglitazone, two key proadipogenic agents. These effects involve direct modulation of PPARγ activity, most likely through regulation of the biosynthesis of PPARγ natural endogenous ligand(s). Together, our data suggest that PBX1 regulates adipocyte development at multiple levels, promoting the generation of NC-derived APs during embryogenesis, while favoring APs proliferation and preventing their commitment to the adipocyte lineage in postnatal life. STEM CELLS *2011;29:1837–1848*

Disclosure of potential conflicts of interest is found at the end of this article.

INTRODUCTION

Obesity and health-related problems, such as cardiovascular disease and type 2 diabetes, are a growing burden for individuals and healthcare systems around the world [1, 2]. Obese individuals are characterized by an excessive expansion of white adipose tissue (WAT). This tissue is the primary site of energy storage in mammals and is mainly composed of white adipocytes that accumulate triglycerides in lipid droplets [3]. Adipose tissue expands as a consequence of increased storage of triglycerides by adipocytes (hypertrophy) or increased adipocyte number (hyperplasia). Since mature adipocytes are postmitotic [4], the generation of new adipocytes throughout life occurs exclusively from differentiation of pre-existing precursor cells [5]. Adipogenesis is generally described as a two-step process: a commitment step, wherein committed adipocyte progenitors (APs or preadipocytes) are generated from multipotent mesenchymal stem cells (MSCs), which also give rise to bones, cartilages, and muscles in response to appropriate developmental signals; and a differentiation step, wherein APs acquire the features of mature, functional adipocytes [3]. Adipose tissue-derived stem cells (ADSCs) constitute postnatal cellular intermediates in this process, which can be isolated from the stromal vascular fraction (SVF) of adipose tissue. In human, ADSCs were isolated from infant adipose tissues and termed "hMADS" for "human multipotent adipose-derived stem" cells [6]. These cells can be expanded in vitro for more than 160 population doublings while maintaining a normal diploid karyotype. However, when stimulated with appropriate signals, they differentiate at a high rate into cells that display properties similar to those of native human adipocytes [7, 8]. hMADS cells therefore constitute a powerful system to investigate human adipogenesis [6, 9, 10].

While adipocyte terminal differentiation has been extensively studied following the derivation of mouse AP cell lines [11–13], very little is known regarding the early steps of adipogenesis. In particular, the molecular mechanisms and the cellular intermediates underlying the transitions from undifferentiated embryonic stem cells (ESCs) to MSCs, and from MSCs to APs, remain unclear, mostly due to lack of specific cell surface markers to define these cells [14]. Recent

Author contributions: M.C.M. and N.B.: conception and design, collection and assembly of data, data analysis and interpretation, and manuscript writing; M.S. and M.L.C.: conception and design, provision of study material, and manuscript writing; C.S. and A.B.: provision of study material, collection and assembly of data, and data analysis and interpretation. C.D.: conception and design, financial support, and manuscript writing. All authors read and approved the final manuscript.

Correspondence: Nathalie Billon, Ph.D., Université de Nice-Sophia Antipolis, CNRS, IBDC, Nice, France. Telephone: 33-04-92-07-69-94; Fax: 33-04-93-37-70-58; e-mail: billon@unice.fr Received June 10, 2011; accepted for publication September 2, 2011; first published online in STEM CELLS *EXPRESS* September 15, 2011. 1066-5099/2009/$30.00/0 doi: 10.1002/stem.737

fluorescence-activated cell sorting (FACS)-based and lineage tracing studies have, however, begun to explore the immunophenotype of postnatal APs in both mice [4, 15] and human [16, 17] WAT. Interestingly, a perivascular signature has been described for MSCs in multiple human organs and a growing body of evidences implicate pericytes as a source of APs in human [18–22]. Finally, the embryonic origin of adipocytes and MSCs, although widely assumed to be exclusively mesodermal, is still a matter of debate. Recently, subpopulations of MSCs and cranial adipocytes were shown to derive from the neuroectoderm through the neural crest (NC) [23, 24].

Mouse ESCs (mESCs) have provided an invaluable system to model the earliest steps of adipocyte development in vitro. Ectodermal, mesodermal, and endodermal derivatives can be generated in vitro by mESCs, following removal of leukemia inhibitory factor and aggregation into embryoid bodies (EBs) [25]. Although mESCs possess a wide spontaneous differentiation potential in vitro [26], they rarely give rise to adipocytes. However, we have shown that an early and transient treatment of EBs with retinoic acid (RA) promotes adipocyte commitment at a high rate [27], providing a unique model to study adipocyte specification. RA receptor β (RARβ) activation is both necessary and sufficient to induce commitment of mESCs into adipocytes, provided that the multifunctional protein kinase glycogen synthase kinase three (GSK3) remains active [28]. The induction of mESC differentiation on single or combined treatment with RARβ agonist and GSK3 inhibitors therefore provides a selective set of screening conditions to uncover the genes involved in the early steps of adipocyte development. We used this powerful comparative system to perform a large-scale gene expression profiling of adipogenesis in mESCs and selected potential early regulators of mESC adipogenesis [29]. Here we describe the functional characterization of one of these candidate genes, the pre-B-cell leukemia transcription factor one (PBX1), in both mESCs and hMADS cells.

Pbx1 belongs to the three-amino acid loop extension class of homeodomain transcription factors, which regulates numerous developmental processes, including morphologic patterning, organogenesis, and hematopoiesis [30–34]. Of note, although PBX1 appears as a global developmental regulator involved in the formation of many organ systems, no role in adipocyte development has been described so far. *Pbx1*$^{-/-}$ mice die in utero at embryonic day 15.5 with severe anemia, spleen aplasia, and skeletal malformations [31, 32]. This precludes the study of the role of *Pbx1* in adipogenesis, which for the most part does not occur until the perinatal period in rodents, and can only be detected macroscopically after birth [35].

In this report, we used complementary loss of function (LOF) approaches and expression studies to investigate the role of PBX1 in two aspects of adipocyte development: its early specification from mESCs and the later proliferation and differentiation of postnatal ADSCs/APs. Our data support novel, stage-specific functions for PBX1 in the control of adipogenesis in both mouse and human.

Materials and Methods

Compounds were bought from Sigma-Aldrich (Lyon, France), unless otherwise indicated.

mESC Culture and Induction of Adipocyte Development

The CGR8 mESC line [36] was used in this study and was maintained as previously described [27, 37, 38]. Commitment to the adipocyte lineage was selectively stimulated through exposure of EBs to CD2314 (a RARβ-selective agonist) or repressed through the addition of (2′*Z*,3′*E*)-6-bromoindirubin-3′-oxime (Bio, a GSK3 inhibitor), or both compounds, between days 3 and 6 [28]. EBs were then plated and treated with 85 nM bovine insulin, 2 nM triiodothyronine, and 0.5 μM rosiglitazone (a *peroxisome proliferator-activated receptor* γ [PPARγ] agonist; GlaxoSmithKline; Marly le Roy, France), from day 7 onward. CD2314 was kindly provided by Prof. Pierre Chambon (Institut de Génétique et de Biologie Moléculaire et Cellulaire, Illkirch, France).

WAT Isolation and Fractionation

Fat tissues were collected from mice and humans under protocols approved by European regulations for the care of research animals and the Institutional Research Board of Inserm and University Hospital Ethics Committee, respectively (supporting information File 1).

hMADS Cell Propagation and Differentiation

hMADS cells were maintained in proliferation medium (PM) composed of Dulbecco's modified Eagle's medium (DMEM) (Invitrogen, Cergy Pontoise, France), 10% fetal calf serum (Dutscher S.A., Brumath, France), 2 mM L-glutamine, 10 mM HEPES buffer, 50 U/ml penicillin, 50 U/ml streptomycin, and 2.5 ng/ml fibroblast growth factor two (FGF2, Peprotech, Neuilly-Sur-Seine, France) [9, 39].

For adipocyte differentiation, hMADS cells were maintained in PM until they reached confluence, when FGF2 was removed. At day 2 postconfluence (designated as day 0), differentiation was induced by addition of differentiation medium (DM) composed of DMEM/Ham's F12 media (50%/50%), 10 μg/ml transferrin, 1 μM dexamethasone (Dex), 0.1 mM 3-isobutyl-1-methylxanthine (IBMX), 5 μg/ml insulin, 0.2 nM triiodothyronine (T3), and 1 μM rosiglitazone. IBMX and Dex were omitted from day 3 onward. The PPARγ antagonist GW9662 was used at 20 μM and was purchased from Cayman (Tallinn, Estonia).

Small Interfering RNA (siRNA) Transfection of hMADS Cells

hMADS cells were transfected by PBX1 siRNA duplexes using HiPerfect reagent (supporting information File 1).

Cell Cycle Analysis

Cell cycle distribution was evaluated using a cyclin A/propidium iodide (PI) double labeling (supporting information File 1).

Assessment of Adipocyte Differentiation

Lipid droplets were visualized after Oil Red O (ORO) staining, as previously described [37, 38]. Enzymatic activity of glycerol-phosphate dehydrogenase (GPDH), an adipocyte-specific enzyme, was measured as previously described [27]. The RNA levels of adipocyte-specific genes were assessed by real-time polymerase chain reaction (PCR).

RNA Isolation and Quantitative Real-Time PCR

Total RNA was extracted using the RNeasy kit (Qiagen, Courtaboeuf, France), and quantitative real-time reverse-transcription PCR analysis was conducted as described previously [23]. Primers sequences are detailed in supporting information File 1.

Western Blot Analysis

Whole cell extracts, sodium dodecyl sulfate–polyacrylamide gel electrophoresis, blotting, and enhanced chemiluminescence were performed as described previously [9] (supporting information File 1).

Statistical Analyses

All biological quantification data are shown as mean values ± SEM of at least three independent experiments and were tested statistically using two-tailed Student's *t* test or *Z* test for location.

Results

Pbx1 Expression Is Induced During Early Adipogenesis in mESCs

Treatment of mESCs with RARβ agonist CD2314 or the GSK3 inhibitor Bio, from days 3–6 after EB formation, is sufficient to drive or inhibit adipocyte development, respectively [28]. Transcriptomic analysis of mESCs identified *Pbx1* as a candidate gene specifically induced in the adipogenic condition [29]. It was selected for further studies because it is widely expressed in mesenchymal tissues during mouse embryonic development [32, 40] as well as in murine and human APs during postnatal life (see below).

The expression levels of *Pbx1* were first assessed in differentiating mESCs by quantitative PCR (qPCR) and Western blot analysis, which confirmed the specific upregulation of *Pbx1* in CD2314-treated EBs (supporting information File 2).

Pbx1$^{-/-}$ mESCs Do Not Develop into Mature Adipocytes

We analyzed adipogenic potential of *Pbx1*$^{-/-}$ mESCs, in which both isoforms of *Pbx1* were inactivated [41]. Adipocyte development was dramatically reduced in *Pbx1*$^{-/-}$ mESCs, as assessed by ORO staining of EB outgrowths at day 21 (Fig. 1A). More than 70% of EB outgrowths contained adipocytes in wild type (WT) cultures induced to differentiate in the presence of CD2314, compared to less than 5% of mutant EB outgrowths in the same condition (Fig. 1B). The inhibition of adipocyte formation was confirmed by measuring GPDH activity (Fig. 1C) as well as quantifying the expression of adipocyte differentiation-specific genes such as *fatty acid-binding protein 4* (*fabp4*), *PPARγ*, *adiponectin*, and *leptin*, which were all substantially reduced in *Pbx1*$^{-/-}$ mESCs (Fig. 1D). Therefore, *pbx1* ablation prevented the development of mature adipocytes in mESCs.

Differentiating *Pbx1*$^{-/-}$ mESCs Do Not Express Early Adipocyte Lineage Markers but Are Not Impaired In Neural Development

The role of PBX1 in the developmental steps that successively operate to transform undifferentiated mESCs into mature adipocytes was further investigated. To monitor the generation of early adipocyte lineage cells from *Pbx1*$^{-/-}$ mESCs, we assessed gene expression at day 11, since it represents the earliest time of appearance of adipocyte lineage-associated factors in this system [27]. As shown in Figure 1D, while *lipoprotein lipase* (*Lpl*) was expressed in CD2314-treated WT mESCs at this stage, reflecting the onset of adipocyte differentiation, this marker was not induced in *Pbx1*$^{-/-}$ mESCs. Interestingly, WT mESCs also expressed *preadipocyte factor 1* (*Pref1*), an AP-associated marker, likely reflecting APs amplification prior to their differentiation (Fig. 1D). In contrast, *Pref1* expression was substantially reduced in *Pbx1*$^{-/-}$ mESCs (Fig. 1D), suggesting that *Pbx1* ablation may have altered the formation and/or the amplification of APs in this system, rather than the subsequent formation of mature adipocytes from these APs per se.

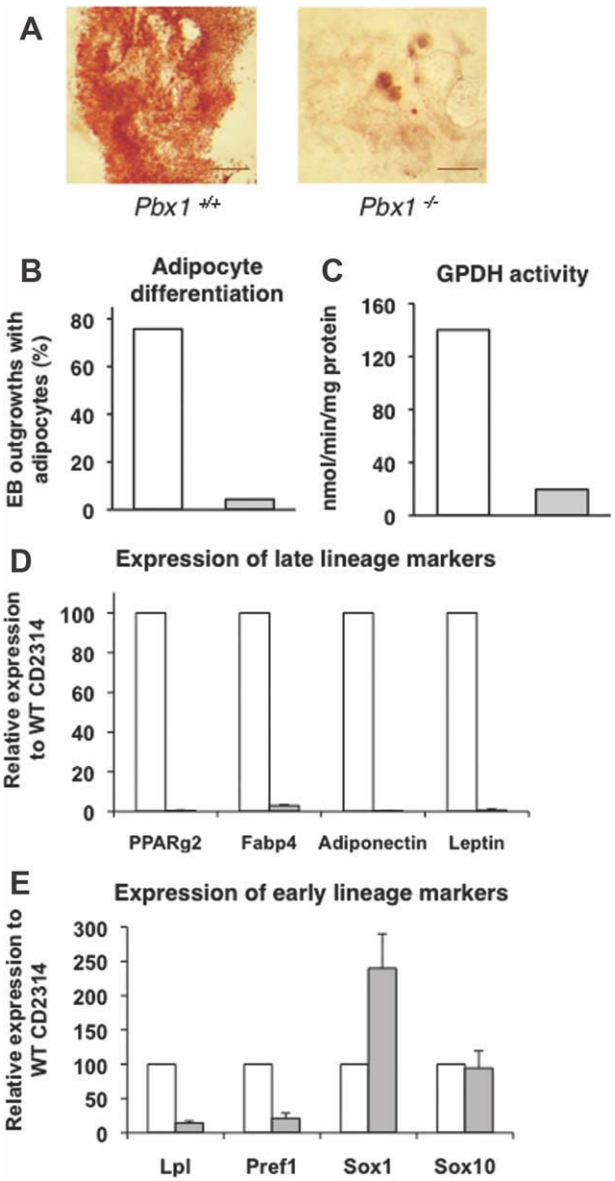

Figure 1. Assessment of adipocyte, neural, and ectomesenchymal development in *Pbx1*$^{+/+}$ and *Pbx1*$^{-/-}$ mouse embryonic stem cells (mESCs). mESCs were successively treated with CD2314 and insulin, rosiglitazone, and triiodothyronine to induce adipogenesis (see Materials and Methods section and supporting information File 2). Adipocyte formation and RNA levels of different lineage markers were assessed at different time points. **(A):** Oil red O staining of EB outgrowths to identify adipocytes (day 21). Scale bar = 1 mm. **(B):** Quantification of the percentage of EB outgrowths with adipocyte colonies (day 21). **(C):** Quantification of GPDH activity (day 21). **(D):** Quantification of late adipocyte markers expression by quantitative polymerase chain reaction (qPCR). The relative expression level of each transcript in *Pbx1*$^{+/+}$ cells treated by CD2314 was considered as 100%. Data are displayed as mean values ± SEM of three independent experiments. **(E):** Quantification of early adipocyte and neural lineage markers expression by qPCR. Data are displayed as in **(D)**. Abbreviations: EB, embryoid body; fabp 4, fatty acid-binding protein 4; GPDH, glycerol-3-phosphate dehydrogenase; lpl, lipoprotein lipase; PPARg2, peroxisome proliferator-activated receptor gamma two; Pref1, preadipocyte factor 1; Sox1, SRY-box containing gene one; WT, wild type.

We previously demonstrated that adipocytes obtained on RA or CD2314 treatment in the mESCs system are mostly derived from a neuroectoderm/NC developmental pathway, rather than a mesoderm-like pathway [23, 28, 29]. Therefore, we analyzed the expression of the neuroectoderm marker *SRY-box containing gene one* (*sox1*) and the NC marker *sox10* in *WT* and *Pbx1*$^{-/-}$ mESCs. As reported previously, both *Sox1* and *Sox10* (Fig. 1E) were successively induced after CD2314 treatment in *WT* mESCs [23]. This induction was not altered in *Pbx1*$^{-/-}$ cells (Fig. 1E), suggesting that neural/NC development normally progressed in this system.

Taken together, these data indicate that the failure of *Pbx1*-deficient mESCs to form mature adipocytes was not due to an impaired neural/NC specification in this system but rather reflected a previously unsuspected role for *Pbx1* in the generation and/or maintenance of NC-derived APs.

PBX1 Is Expressed in Postnatal Adipose Tissues and in hMADS Cells

Although mESCs offer a unique model to study the ontogeny of the adipocyte lineage during embryogenesis, this system suffers from an inherent heterogeneity and is still lacking specific cell surface markers for the isolation of pure populations of embryonic APs [14]. Furthermore, primary APs cannot be derived from either murine or human embryos due to the late development of the murine adipose organ and ethical reasons, respectively. To study the potential role of PBX1 in APs biology during postnatal life, its expression was first assessed in native WAT from both mice and human. To discriminate between the distinct cell populations composing this tissue, that is, APs, immune cells and endothelial cells, all present in the SVF, and mature adipocytes, an immunoselection/depletion approach was used. This strategy previously identified resident APs within the CD34^{+}/CD31^{-} fraction of human WAT. As shown in Figure 2A, the highest levels of *PBX1* expression could be detected in APs. Immune cells, endothelial cells, and mature adipocytes also expressed PBX1, although to a lesser extent. Similarly, *Pbx1* expression was detected in native mouse adipose tissue, where it was enriched in the SVF, consistent with a role for Pbx1 in the regulation of the early steps of postnatal adipogenesis (Fig. 2B).

To further dissect out the role of *PBX1* in postnatal AP proliferation and differentiation, we used hMADS cells, which constitute a powerful system to investigate human adipogenesis [6–10]. As shown in Figure 2C, *PBX1* was expressed by proliferating, undifferentiated hMADS cells (EXPO). Expression levels increased slightly when hMADS cells were grown to confluence (a prerequisite for adipocyte differentiation), reached a maximum 2 days after induction of adipocyte differentiation (day 2) and then moderately decreased throughout the differentiation period. All together, these expression data suggest that *PBX1* could be involved in postnatal adipogenesis and might regulate both AP proliferation and differentiation.

Silencing of *PBX1* Expression Inhibits Proliferation of hMADS Cells

A siRNA-mediated gene silencing approach was used to investigate the role of *PBX1* in postnatal AP proliferation. hMADS cells were independently transfected with two nonoverlapping *PBX1* siRNAs, maintained in transfection medium for 1 day and grown in PM for 5 days. Efficient inhibition of *PBX1a* and *PBX1b* expression was obtained using this approach (Fig. 3A). Cell numbers were measured at various time points after siRNAs transfection. As shown in Figure 3B, *PBX1* silencing significantly decreased hMADS cell numbers when compared to nonsilenced conditions. Of note, *Pbx*1

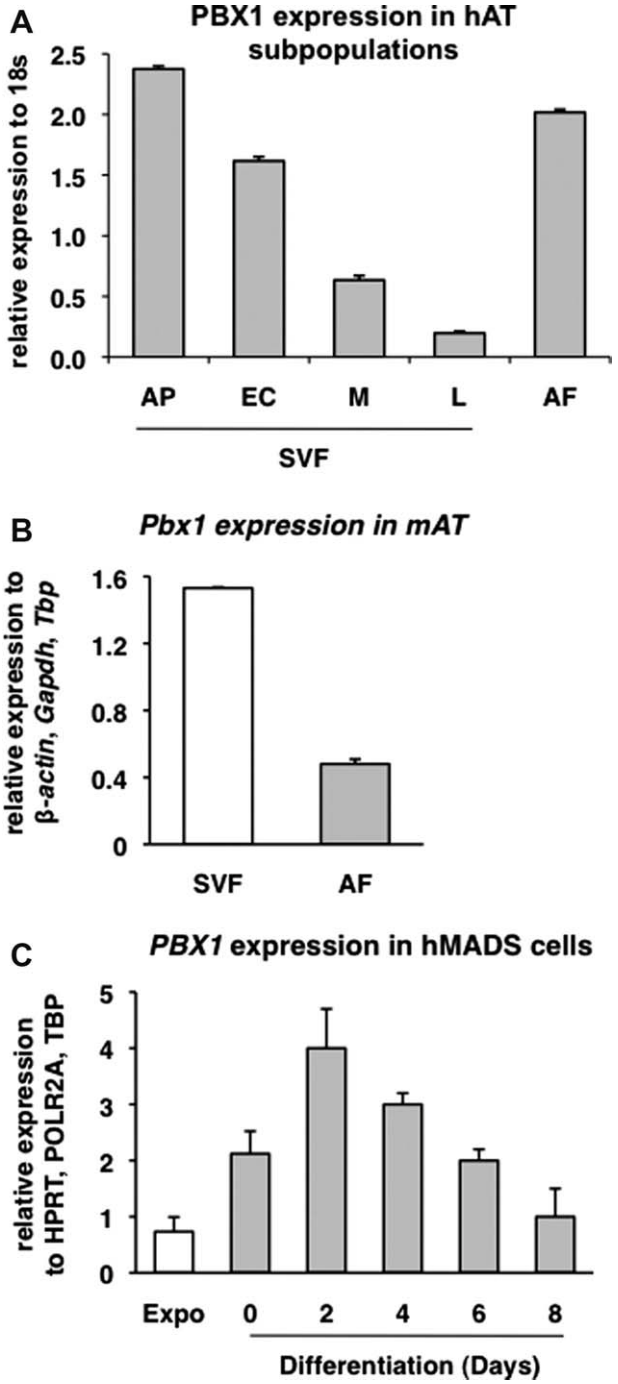

Figure 2. Relative expression of *PBX1* in postnatal adipose tissues and hMADS cells. **(A):** hAT was obtained from 15 patients (18.4 < body mass index [BMI] <42.5). hAT was fractionated using an immunoselection strategy and *PBX1* expression was assessed by quantitative polymerase chain reaction in the indicated cell subpopulations. **(B):** *Pbx1* expression in fractionated periepididymal mAT isolated from 10-week-old mice. **(C):** *PBX1* expression in proliferating (EXPO), confluent (0), or differentiating hMADS cells. Data are displayed as mean values ± SEM of three independent experiments. Abbreviations: AF, adipocyte fraction; AP, adipocyte progenitors; EC, endothelial cells; hMADS, human multipotent adipose-derived stem; hAT, human adipose tissue; L, lymphocytes; M, macrophages; mAT, mouse adipose tissue; PBX1, pre-B-cell leukemia transcription factor one; SVF, stromal vascular fraction.

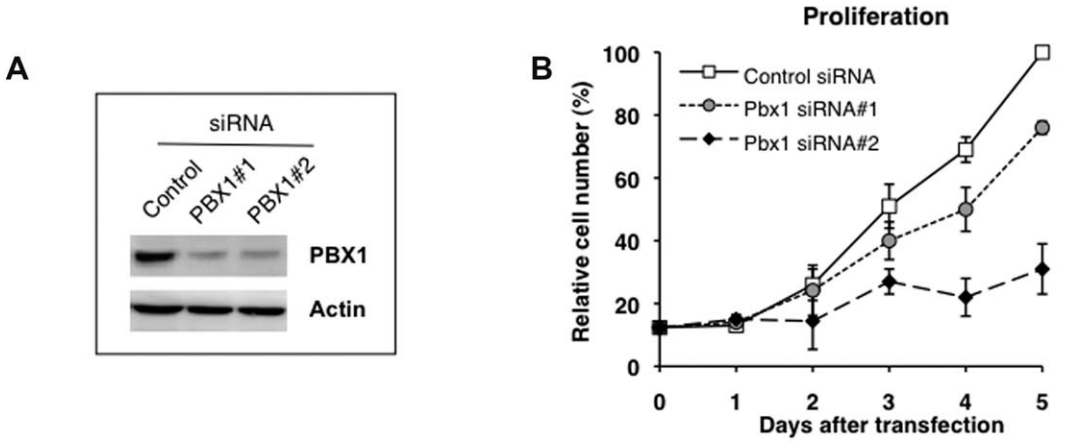

C

Cell cycle analysis	G0/G1	S/G2	M
Proliferating cells	63.5%	32.1%	3.6%
No FCS 48H			
Control siRNA	89%	5.9%	4.3%
PBX1 #1 siRNA	89.6%	4.9%	5%
PBX1 #2 siRNA	88.8%	5.3%	5.4%
Restim FCS 24h			
Control siRNA	80.9%	14.7%	3.7%
PBX1 #1 siRNA	88.5%	6.8%	4%
PBX1 #2 siRNA	89.2%	5.7%	4.1%

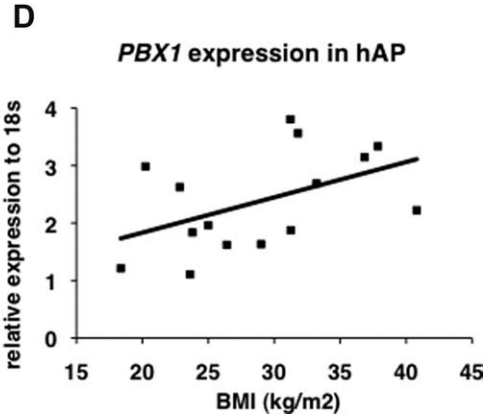

Figure 3. Effect of *PBX1* silencing on human multipotent adipose-derived stem (hMADS) cells proliferation *PBX1* and correlation of *PBX1* expression with BMI in hAT. **(A–C):** hMADS cells were transfected with either scrambled (control) siRNA, or two different siRNAs directed against *PBX1*. They were then either maintained under proliferating conditions **(A** and **B)** or synchronized by serum deprivation for further cell cycle analysis **(C)**. **(A):** Protein levels of PBX1b and actin were assessed by Western blotting 3 days after transfection. **(B):** Cell numbers were measured at indicated time points in proliferating conditions. Data are displayed as mean values ± SEM of three independent experiments. **(C):** Cell cycle distribution was evaluated by flow cytometry analysis of cyclin A/propidium iodide double staining in proliferating hMADS, hMADS cells synchronized by FCS deprivation, or hMADS cells restimulated in 0.5% FCS + 2.5 ng/ml fibroblast growth factor two. Percentages of cells in G0/G1, S/G2, or M phases of the cell cycle were quantified and are indicated in the table. Data are presented as the results of a typical experiment (see supporting information File 3 for more details). **(D):** *PBX1* expression in the adipocyte progenitor (AP) fraction of hAT as a correlation to BMI. hAT was obtained from 15 patients (18.4 < BMI <42.5) and was fractionated using an immunoselection strategy. *PBX1* expression in the AP fraction was assessed by quantitative PCR and expressed as a function of BMI. *PBX1* expression in AP was found to be positively correlated to BMI ($p = .036$, Pearson $r = .5$). Abbreviations: BMI, body mass index; FCS, fetal calf serum; hAT, human adipose tissue; siRNA, small interfering RNA.

silencing had no effect on cell death by necrosis or apoptosis, as investigated using an annexin V–fluorescein isothiocyanate/PI assay (data not shown). These data indicate that PBX1 could play a crucial role in the maintenance of AP proliferation during postnatal stages.

To investigate the mechanisms by which *PBX1* silencing reduced hMADS cells proliferation, its effect on cell cycle distribution was evaluated using a cyclin A/PI double labeling flow cytometry assay (Fig. 3C and supporting information File 3). hMADS cells were transfected with control or *PBX1* siRNAs and synchronized through a 48H serum deprivation, resulting in more than 88% of cells arrested in G0/G1. Cells were then restimulated for 24 hours in 0.5% serum. As expected, cells transfected with the control siRNA re-entered cell cycle, displaying a significant increase in the number of cells in the S phase (14.7% compared to 5.8% before restimulation) and a concomitant decrease in cells blocked in G0/G1. In contrast, hMADS cells transfected with *PBX1* siRNAs maintained a high proportion of cells in G0/G1 and failed to re-enter into the S phase.

Together, these data suggest that PBX1 might normally help maintaining a pool of proliferative APs within human adipose tissue (hAT). The expression of *PBX1* was therefore investigated in the AP fraction of hAT from patients with different body mass index (BMI). Interestingly, *PBX1* expression was positively correlated to the BMI of both lean/overweight (BMI <30 kg/m^2) and obese (BMI >30 kg/m^2) subjects (Fig. 3D) suggesting that it might constitute a new indicator of APs proliferation in normal and pathological adipose tissue in human.

Silencing of *PBX1* Expression Promotes Adipocyte Differentiation of hMADS Cells

To investigate the role of PBX1 on hMADS cell differentiation toward the adipocyte lineage, hMADS cells were grown to confluence, transfected with *PBX1* siRNAs, and maintained for 2 days before adipocyte differentiation was induced (a time point hereafter referenced as "day 0"). *PBX1* silencing had a pronounced stimulating effect on adipocyte differentiation. By day 9, *PBX1*-silenced cultures displayed a substantial

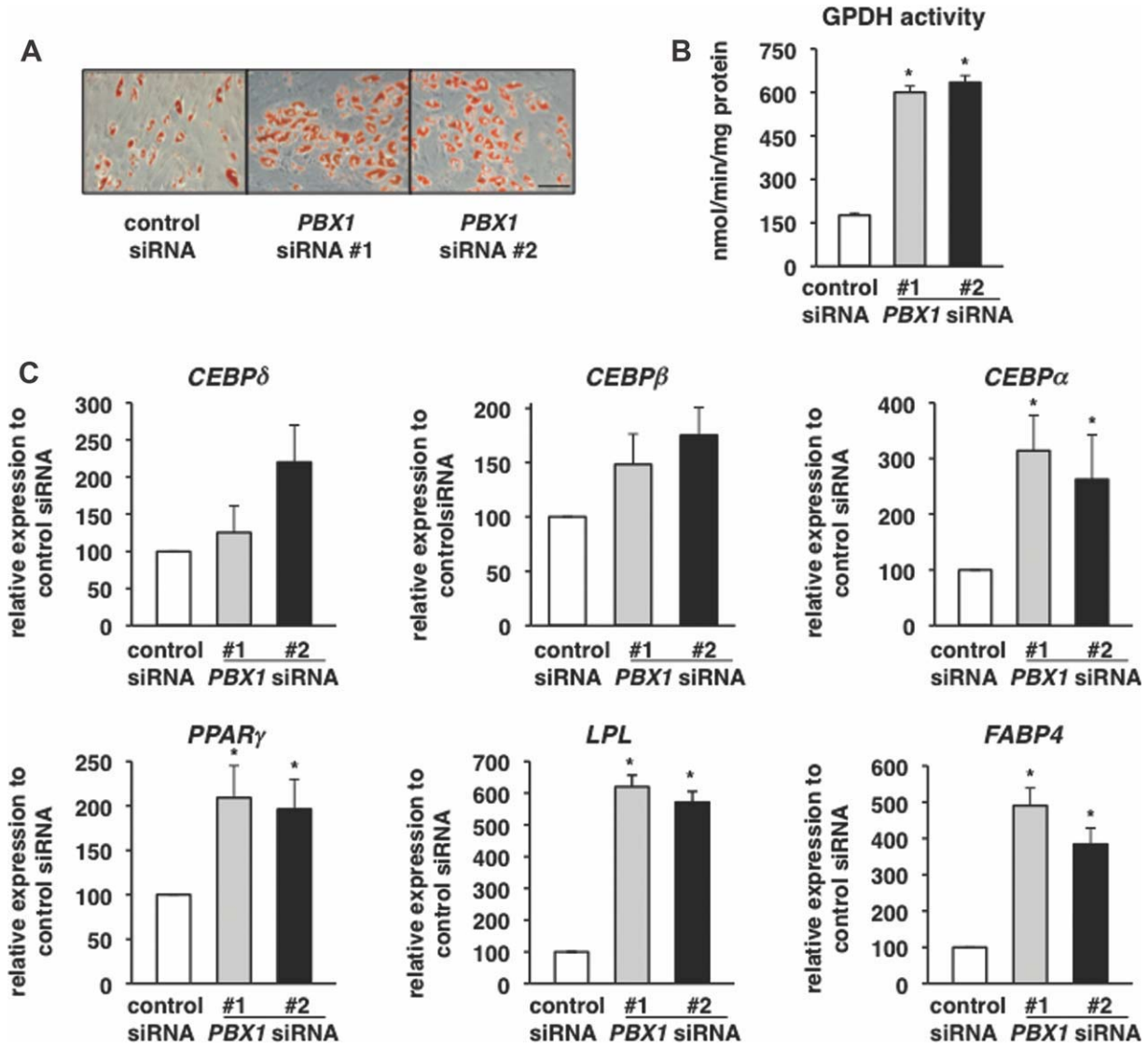

Figure 4. Effect of *PBX1* silencing on human multipotent adipose-derived stem (hMADS) cells differentiation. Confluent hMADS cells were transfected as described in Figure 3 and adipocyte differentiation was induced 2 days post-transfection (day 0). **(A):** Adipocytes were identified by Oil red O staining at day 9 after induction of differentiation. Scale bar = 100 μm. **(B):** Quantification of GPDH activity at day 9. **(C):** Quantification of *C/EBPδ*, *C/EBPβ*, *C/EBPα*, *PPARγ*, *LPL*, or *FABP4* RNA expression by quantitative polymerase chain reaction at day 3. The relative expression level of each RNA in cells transfected with control siRNA was considered as 100%. Data are displayed as mean values ± SEM of three independent experiments. *Indicates values that were found to be significantly different from the control siRNA condition using statistical *Z*-test ($p < .05$). Abbreviations: C/EBP, CCAAT/enhancer binding protein; FABP4, fatty acid-binding protein 4; GPDH, glycerol-3-phosphate dehydrogenase; LPL, lipoprotein lipase; PBX1, pre-B-cell leukemia transcription factor one; PPARγ, peroxisome proliferator-activated receptor gamma; siRNA, small interfering RNA.

increase in adipocyte numbers (Fig. 4A). Accordingly, GPDH activity levels were strongly increased in these cells (Fig. 4B).

To dissect out the role of *PBX1* in the earliest steps of the postnatal adipocyte differentiation program, the expression of adipocyte differentiation regulators was analyzed in hMADS cells transfected with *PBX1* siRNAs. As shown in Figure 4C, by day 3 of differentiation, the RNA levels of *FABP4* and *LPL* were already significantly increased in silenced hMADS cells, indicating that *PBX1* acts at the very onset of adipocyte differentiation in human APs. Interestingly, the stimulation of adipocyte differentiation by *PBX1* siRNAs was only accompanied with a moderate rise in *PPAR gamma* (*PPARg*) and *CCAAT/enhancer binding protein alpha* (*C/EBPα*) expressions (Fig. 4C), while *C/EBPβ* and *C/EBPδ*, the two main regulators of *PPARγ* expression during adipogenesis, were not found to be significantly modulated in these conditions (Fig. 4C). Together, these data indicate that *PBX1*-mediated regulation of adipocyte differentiation might not involve a direct regulation of the expression of adipogenesis master regulators.

To examine/rule out the possibility that the contrasting effects of PBX1 LOF in mESCs versus hMADS cells might reflect species differences, we next assessed these effects in mouse embryonic fibroblasts (MEFs) isolated from $Pbx1^{+/+}$ and $Pbx1^{-/-}$ developing embryos (supporting information File 4). Strikingly, $Pbx1^{-/-}$ MEFs showed a significant increase in adipocyte differentiation, as measured by ORO staining, GPDH activity and the expression of adipocyte differentiation markers. Therefore, similarly to what was observed in

hMADs cells using an alternative silencing method, the absence of *Pbx1* promoted adipocyte differentiation in MEFs.

Silencing of *PBX1* Expression Can Substitute For Glucocorticoids- and Rosiglitazone-Induced Adipocyte Differentiation of hMADS Cells

Adipocyte differentiation of human adipose stem cells can be induced in vitro by exposition to a cocktail of adipogenic inducers containing insulin, glucocorticoids (such as Dex), agents that elevate cAMP (such as the phosphodiesterase inhibitor IBMX), and T3 [6, 34]. This treatment launches a transcriptional cascade that converges on the expression of PPARγ, which functions as the master regulator of adipogenesis in vitro and in vivo. Once initiated, this program becomes independent of Dex and IBMX but requires exogenous addition of PPARγ synthetic ligand activators, such as rosiglitazone (Rosi), for adipogenesis to proceed, as endogenous PPARγ ligands remain unknown and do not appear to be produced in hMADS cells [42, 6].

To investigate the mechanisms of actions of PBX1 in adipogenesis, we tested whether the partial ablation of *PBX1* could substitute for any component of the DM mentioned above or could be sufficient to induce adipocyte differentiation on its own. For this, hMADS cells transfected with *PBX1* siRNAs were exposed to complete DM, DM depleted from individual adipogenic component, or DM depleted from all adipogenic compounds (−DM). Adipocyte differentiation was assessed by direct visualization of lipid-containing adipocytes (Fig. 5A) and by monitoring GPDH activity (Fig. 5B) and gene expression specific to adipocytes (Fig. 5C). As reported in Figure 5, insulin, T3, and IBMX were individually dispensable for adipocyte development of hMADS cells (see the "control siRNA" lane and bars). In contrast, Dex and Rosi were both necessary for complete adipogenesis, as neither mature adipocytes nor GPDH activity could be observed in cell cultures deprived from these factors (see "control siRNA," "−Dex," and "−Rosi"). Silencing of *PBX1* expression was not sufficient to promote adipocyte differentiation in the absence of any adipogenic inducers (see "*PBX1* siRNA" and "−DM"). However, it could compensate, at least in part, for the absence of Dex and Rosi, as indicated by the presence of adipocytes, GPDH activity, and re-expression of adipocyte differentiation markers in cultures deprived of these factors but transfected by *PBX1* siRNAs (see "*PBX1* siRNA," "−Dex," and "−Rosi").

Again, although the pronounced stimulation of adipocyte differentiation by *PBX1* siRNAs in DM, −Dex, and −Rosi conditions was associated to a strong increase in the expression of *FABP4* and *Adiponectin*, two PPARγ target genes, it was only accompanied with a moderate rise in *PPARγ* expression itself (Fig. 5C), suggesting that PBX1 effects might reflect regulation of PPARγ activity rather than expression.

PBX1 Silencing-Induced Adipocyte Differentiation Is Mediated by a Direct Control on PPARγ Activity

To test the hypothesis that PBX1 might control adipocyte differentiation through direct modulation of PPARγ activity, as suggested by the above experiments, we first checked that the rescue of adipocyte differentiation by *PBX1* silencing in the absence of Rosi could be attributed to a specific effect on PPARγ activity. hMADS cells transfected with *PBX1* siRNAs were exposed to a selective PPARγ ligand antagonist (GW9662) and subjected to adipocyte differentiation in the absence of Rosi. As shown in Figure 6, *PBX1* silencing was no longer able to rescue adipocyte differentiation in these conditions, indicating that PBX1 effects selectively depend on PPARγ activation.

The partial rescue of adipogenesis by PBX1 silencing in the absence of Rosi suggests that PBX1 might regulate PPARγ activity by controlling the biosynthesis of PPARγ natural endogenous ligand(s), alleviating the need for exogenous addition of PPARγ synthetic ligand activators. Although PPARγ natural ligand activator(s) remain uncharacterized at present, they belong to the fatty acids family, which are biosynthesized from their precursor, arachidonic acid (ARA). To test the hypothesis that *PBX1* might be involved in PPARγ activation by endogenous fatty acids, we assessed whether addition of ARA could have a cooperative effect on *PBX1* silencing-mediated stimulation of adipocyte differentiation in the absence of Rosi. As shown in Figure 6A, ARA was not able on its own to induce full adipocyte formation in the absence of Rosi (see "control SiRNA" and "−Rosi+ARA"), confirming the observation that PPARγ endogenous ligand(s) activators are not produced in hMADS cells [6]. However, ARA strongly potentiated *PBX1* siRNA-mediated induction of adipocyte differentiation in the absence of Rosi (Fig. 6). All together, these observations suggest that *PBX1* silencing-mediated induction of adipocyte differentiation might involve, at least in part, stimulation of PPARγ activity through synthesis of its endogenous ligand(s) activators.

Discussion

The signaling and transcriptional networks that regulate the early steps of adipocyte development remain largely unknown. We have recently performed a genome-wide transcriptomic analysis of adipogenesis in mESCs and revealed a plethora of novel candidate genes for adipocyte development, a large proportion of which had no previous link to adipocyte biology [29]. In this study, we demonstrate novel, stage-specific roles for the PBX1 transcription factor in regulating the early steps of adipocyte development in both mESCs and human adipose stem cells. This is the first report involving PBX1 in adipogenesis.

As *Pbx1*-deficient mice die at E15.5 before the formation of adipose tissue, we first assessed the effect of *Pbx1* LOF in *pbx1*$^{-/-}$ mESCs and demonstrated that embryonic adipocyte development was strongly inhibited in the absence of Pbx1. Of note, adipocytes obtained on RA or CD2314 treatment of mESCs are mostly derived from a neuroectoderm/NC pathway rather than a mesodermal pathway [23]. Using NC lineage cell-fate mapping in transgenic mice, we previously confirmed the relevance of these findings in vivo by showing that a subset of cranial adipocytes indeed derived from the NC, and not from the mesoderm, during normal development [23]. In this study, we showed that the failure of *pbx1*$^{-/-}$ mESCs to generate mature adipocytes was unlikely due to prior impaired neural/ectomesenchymal specification but rather reflected a previously unsuspected role for *Pbx1* in the early steps of adipocyte development. In accordance with our findings, PBX1 was recently shown to be dispensable for neural commitment of RA-treated mESCs [43]. The finding that *Pbx1* is expressed in various mesenchymal compartments during embryogenesis is consistent with its function in the early steps of adipogenesis. Interestingly, at E11.5, *Pbx1b* is expressed in the mesenchyme of the second branchial arch (BA2), which is known to derive from the cranial NC, and *Pbx1*$^{-/-}$ embryos display an anterior transformation of BA2-derived skeletal structures into elements reminiscent of BA1-derived cartilages [32]. The work presented here suggests that

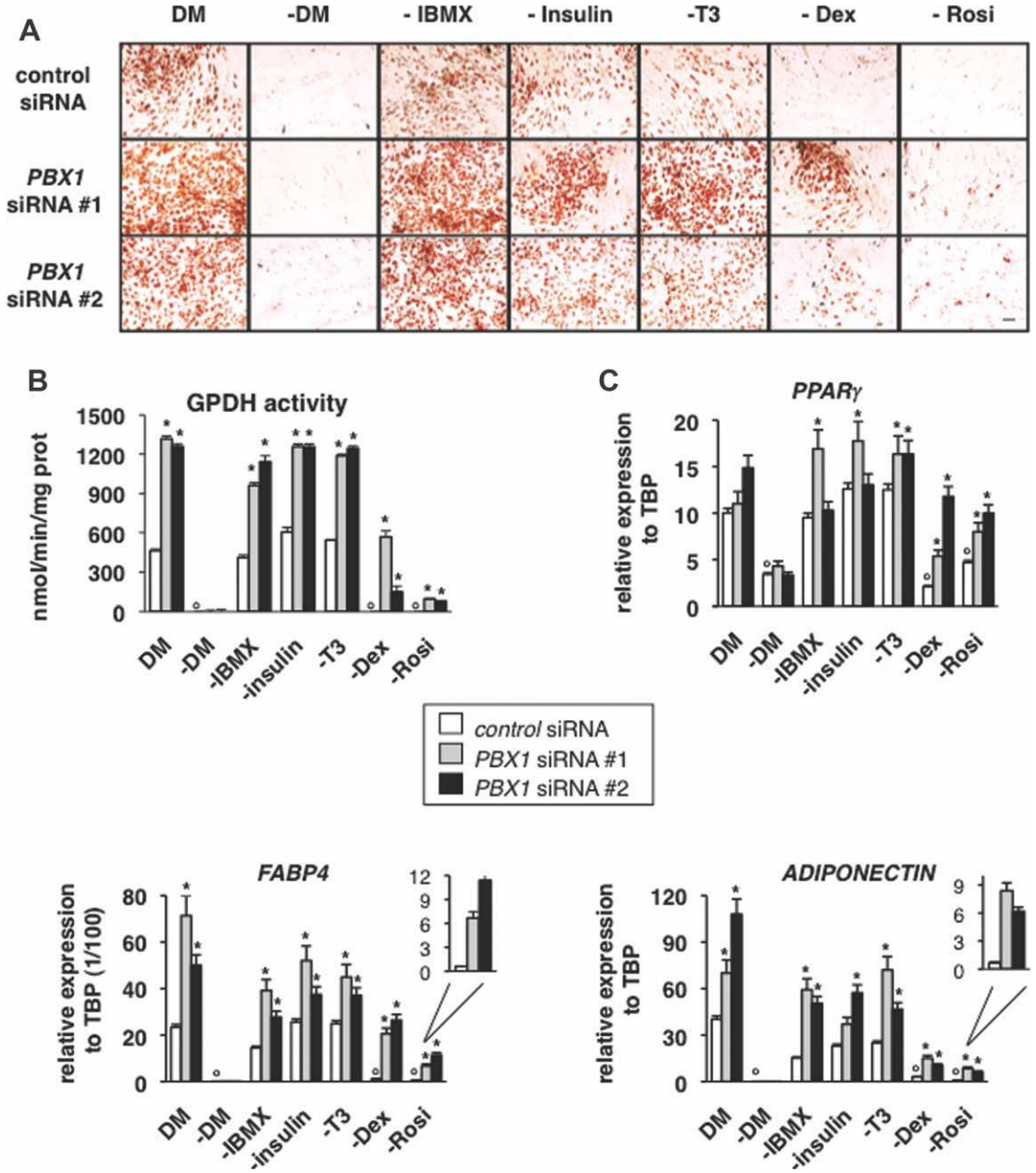

Figure 5. Effect of *PBX1* silencing on human multipotent adipose-derived stem (hMADS) cell response to adipogenic signals. Confluent hMADS cells were transfected as described in Figure 3. After 2 days, they were exposed to complete DM, DM depleted from the indicated adipogenic component, or control medium depleted from all adipogenic components (−DM). **(A):** Identification of adipocytes by Oil Red O staining (day 11). Scale bar = 100 μm. **(B):** Quantification of GPDH activity (day 11). **(C):** Quantification of *PPARγ* and *FABP4* (day 6), and *ADIPONECTIN* (day 9) RNA levels by quantitative polymerase chain reaction. For the sake of clarity, relative expressions were divided by 100 for *FABP4*. Data are displayed as mean values ± SEM of three independent experiments. °Indicates control siRNA values that were found to be significantly different from the complete DM condition using statistical *t* test ($p < .05$). *Indicates PBX1 siRNA values that were found to be significantly different from the control siRNA in the same medium condition using statistical *t* test ($p < .05$). Abbreviations: Dex, dexamethasone; DM, differentiation medium; FABP4, fatty acid-binding protein 4; GPDH, glycerol-3-phosphate dehydrogenase; IBMX, 3-isobutyl-1-methylxanthine; PBX1, pre-B-cell leukemia transcription factor one; PPARγ, peroxisome proliferator-activated receptor gamma; Rosi, rosiglitazone; T3, triiodothyronine; siRNA, small interfering RNA.

Pbx1 likely serves an important role in the generation and/or maintenance of NC-derived APs and opens new avenues to study the transcriptional networks underlying this process.

Our data further indicate that the role of PBX1 is not restricted to NC-derived adipogenesis, however. Indeed, in addition to its expression in NC-derived mesenchyme, we could also detect *Pbx1* in the progenitor compartment of postnatal, truncal adipose tissues (that do not arise from the NC [23] in mice. In addition, PBX1 was expressed in the native APs fraction of hAT as well as in human APs derived from the inguinal fat pad of young infants (hMADS cells). We show that silencing of *PBX1* in these cells sharply reduced their proliferation and promoted precocious adipocyte differentiation, suggesting that this factor normally negatively regulates the switch from proliferation to differentiation in postnatal APs. Of note, the apparently contrasting effects of PBX1 LOF in

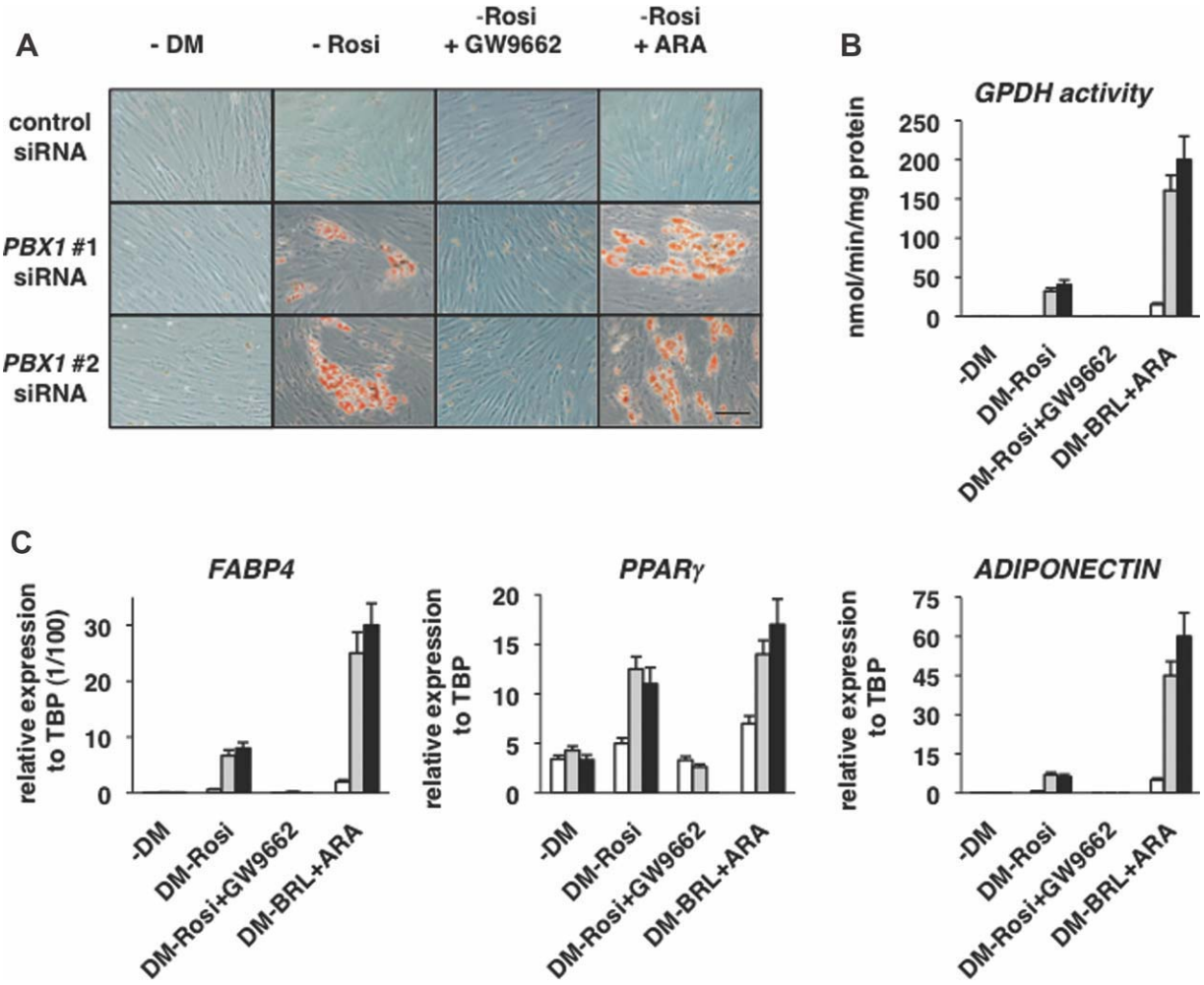

Figure 6. Effect of a selective PPARγ antagonist (GW9662) and ARA on *PBX1* silencing-mediated rescue of adipocyte differentiation in the absence of Rosiglitazone. Confluent human multipotent adipose-derived stem (hMADS) cells were transfected as described in Figure 3. After 2 days, they were exposed DM depleted from any adipogenic component (−DM)), DM depleted from rosiglitazone (DM−Rosi), or DM depleted from Roziglitazone but supplemented with 20 μM GW9662 (DM−Rosi+GW9662). **(A):** Identification of adipocytes by Oil red O staining at day 11. Scale bar = 100 μm. **(B):** Quantification of *PPARγ*, *FABP4*, and *ADIPONECTIN* RNA levels by quantitative polymerase chain reaction (day 9). Data are displayed as mean values ± SEM of three independent experiments. Abbreviations: ARA, arachidonic acid; DM, differentiation medium; FABP4, fatty acid-binding protein 4; GPDH, glycerol-3-phosphate dehydrogenase; PBX1, pre-B-cell leukemia transcription factor one; PPARγ, peroxisome proliferator-activated receptor gamma; Rosi, rosiglitazone; siRNA, small interfering RNA.

mESCs and hMADS cells could not be attributed to species or methodologies differences, as both *PBX1*-silenced hMADs cells and *Pbx1*$^{-/-}$ MEFs displayed increased adipocyte differentiation. Therefore, the absence of adipocyte differentiation in *Pbx1*$^{-/-}$ mESCs rather reflects prior defect in APs specification or amplification. As our data in hMADS cells suggest that PBX1 plays a crucial role for APs proliferation, it is conceivable that APs may still be produced from *Pbx1*$^{-/-}$ mESCs but prematurely exit cell cycle, precluding their expansion and further response to adipogenic signals. We could not directly assess the effect of *pbx1* ablation on the proliferation and cell cycle of mESC-derived APs. Indeed, as mentioned earlier, this system is still lacking specific cell surface markers for the isolation of pure AP populations. While recent FACS-based and lineage tracing in vivo studies shed new light on the molecular signature of postnatal APs in mouse [4, 15] and human [16–22], some pointing at pericytes as a potential source of human APs, these new markers appear to be widely expressed in differentiating mESCs and therefore might not be appropriate to isolate discrete population of APs in this system (unpublished data). For these reasons, we deliberately choose to further dissect out the role of PBX1 on AP proliferation and differentiation in the homogeneous hMADS cell model, which so far has no murine counterpart.

The findings that silencing of *PBX1* expression in hMADS cells inhibits their proliferation indicate that PBX1 might play an important role in the maintenance of a proliferative state in postnatal APs. Interestingly, PBX1 has been implicated in promoting progenitor cell expansion at the detriment of differentiation in multiple developing organs. For instance, *Pbx1*$^{-/-}$ embryos are affected by severe anemia, which was attributed to decreased proliferation of hematopoietic progenitors [31]. Furthermore, *Pbx1*-deficient embryonic chondrocytes display diminished proliferation and accelerated differentiation, resulting in several skeletal malformations [32]. Finally, loss of *Pbx1* function during spleen formation has been associated with a reduction of progenitor cell proliferation and failed expansion of the splenic anlagen [44]. The present report indicates that, similarly to other organs, PBX1 might also help to maintain the pool of proliferative progenitors in the adipose tissue. Interestingly, we also report a positive correlation

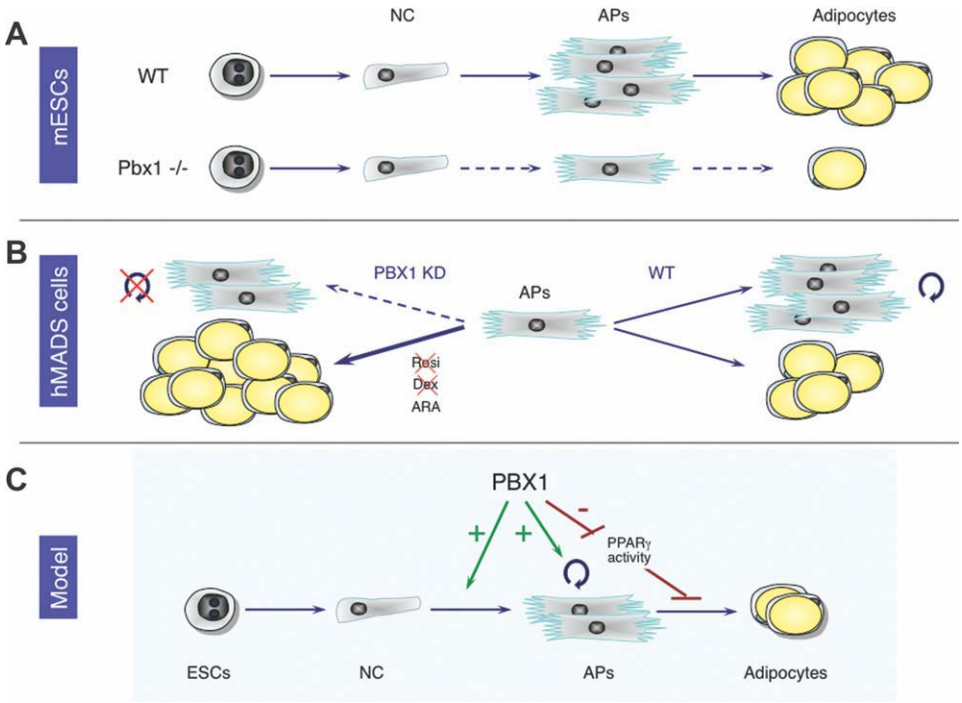

Figure 7. Summary of mESCs and hMADS findings and schematic model for PBX1 roles during adipogenesis. **(A)**: *Pbx1*$^{-/-}$ mESCs neither develop into mature adipocytes nor express early adipocyte lineage markers, while showing no impairment in neural crest specification. **(B):** Silencing of *PBX1* in hMADS cells reduces their proliferation and inhibits their cell cycle, while it promotes their differentiation toward the adipocyte lineage and can partially substitutes for key proadipogenic agents such as Dex, and Rosi. These effects are potentiated by ARA, a fatty acid precursor. **(C):** Altogether, our data suggest a model in which PBX1 regulates adipogenesis at multiple levels: during embryogenesis, PBX1 promotes the generation and/or the expansion of APs from the neural crest development pathway. In postnatal life, PBX1 favors AP proliferation and prevent their differentiation toward the adipocyte lineage by interfering with the activity of the master regulator PPARγ, preventing the biosynthesis of its unknown, natural endogenous ligand(s). Abbreviations: APs, adipocyte progenitors; ARA, arachidonic acid; Dex, dexamethazone; hMADS, human multipotent adipose-derived stem; KD: knock down; mESCs, mouse embryonic stem cells; NC, neural crest; PBX1, pre-B-cell leukemia transcription factor one; PPARγ, peroxisome proliferator-activated receptor gamma; Rosi, rosiglitazone; WT, wild type.

between the expression of *PBX1* in the AP fraction of human WAT and the increase in fat mass observed when comparing lean, overweight, and obese subjects. The excessive development of WAT has been associated to an increase in both adipocyte size and numbers, the latter phenomenon resulting from the recruitment of an existing pool of APs. Recently, the AP fraction of human WAT has been shown to contain proliferating cells, the proportion of which increased in obese patients [45], suggesting that fat mass expansion might result, in part, from the proliferation of a resident pool of APs. As we report here that PBX1 may promote APs proliferation in the hMADS cell system, it is tempting to speculate that the rise of *PBX1* expression in APs with BMI reflects an increased proliferation of APs in the adipose tissue of obese patients. In this regard, PBX1 might represent a novel regulator of the size of the AP pool in hATs in both normal and pathological situations. In line with this hypothesis, PBX1 polymorphisms have recently been associated with overweight/obesity in the Korean population [46].

In addition to its effect on hMADS proliferation, *PBX1* silencing resulted in a sharp and rapid stimulation of adipocyte differentiation, suggesting that PBX1 might prevent the onset of adipocyte differentiation by directly repressing the expression of immediate early transcriptional regulators of adipocyte commitment such as C/EBPδ and C/EBPβ, which converge on the induction of the expression of PPARγ, the master regulator of adipogenesis. However, we report here that the expression of these master regulators was not (*C/EBPδ* and *C/EBPβ*) or only moderately (*PPARγ*) increased in *PBX1*-silenced hMADS cells and provide evidences that PBX1 might control adipocyte differentiation through direct modulation of PPARγ activity. Indeed, by uncoupling the proadipogenic activities of the signaling molecules normally used to induce differentiation of hMADS cells, we demonstrate that *PBX1* silencing promotes adipogenesis in the absence of exogenous addition of the synthetic PPARγ ligand activator rosiglitazone, an effect that could not be attributed to the sole regulation of early adipogenesis regulators expression by PBX1. The effect of *PBX1* silencing on the conversion of hMADS cells into adipocytes in hMADS cells in the absence of rosiglitazone, although partial, was PPARγ-specific, as it could be counteracted by a selective PPARγ antagonist (GW9662).

We further investigated the mechanisms by which PBX1 might control PPARγ activity and adipocyte differentiation. The observation that *PBX1* silencing limited the need for exogenous addition of PPARγ synthetic ligand activators for adipocyte differentiation prompted us to investigate whether PBX1 might regulate PPARγ activity by controlling the biosynthesis of PPARγ natural endogenous ligand(s), which are not normally produced by hMADS cells. We report that the fatty acid precursor ARA strongly potentiated *PBX1* silencing-mediated stimulation of adipocyte differentiation in hMADS cells, suggesting that PBX1 may normally interfere with PPARγ activity by preventing the biosynthesis of its unknown, natural endogenous ligand(s). Further studies will have to determine at which steps of this complex biosynthesis pathway PBX1 might act, and how. Interestingly, *PBX1*

silencing might provide an ideal biological setting for the so far unsuccessful quest for PPARγ natural endogenous ligand(s).

Conclusion

In summary, the data we report here suggest novel, stage-specific roles for PBX1 in controlling two pivotal aspects of adipocyte development, which are summarized on a schematic model (Fig. 7). During embryogenesis, PBX1 might promote the specification of APs from the NC development pathway and their amplification prior to differentiation. In postnatal life, PBX1 might favor AP amplification through cell division and prevent their differentiation by interfering with the activity of PPARγ, the master regulator of adipogenesis. Adipose tissue-specific conditional knockdown of *pbx1* in mice should help to further unravel the dual function of PBX1 during adipogenesis. As *PBX1* expression in APs of human patients was found here to be correlated to their BMI, it will now also be of crucial importance to investigate how PBX1 is regulated in the adipose organ of normal versus obese individuals, and whether it could constitute a potential target for controlling the size of the AP pool in normal and pathological situations, such as obesity. Finally, a substantial body of work has linked adipogenesis to circadian clock, a pathway that involves GSK3β and orphan nuclear hormone receptors (RORs), which are closely related to RARs. As PBX1 was derived from a comparative transcriptomic analysis involving RAR agonists and GSK3 inhibitors, it is intriguing that PBX2, a PBX1-related family member, was found to be an oscillating gene conserved across liver, white, and brown adipose tissues [47]. Investigation of the potential implication of PBX1 in the relationship between adipogenesis and circadian mechanisms might therefore unravel another unsuspected function for PBX1 in adipocyte biology.

Acknowledgments

We thank Agnes Loubat for help on the Pasteur flow cytometry platform; Pauline Decaunes for her technical assistance; and G. Ailhaud, Z. Amri, D. Pisani, and M. Djedaini for sharing data and providing helpful insight into this work. This research was supported by CNRS, by the Sixth Research Framework Programme of the European Union (Project FunGenES LSHG-CT-2003—503494) and the Egide Parrot PHC Programme No 20679QJ. M.C.M. was supported by an Early-Stage Research Training Host Fellowship action of the EU Marie Curie program and the Portuguese Foundation for Science and Technology (SFRH/BD/44625/2008, financed by POPH–QREN).

Disclosure of Potential Conflicts of Interest

The authors indicate no potential conflicts of interest.

References

1 Kahn SE, Hull RL, Utzschneider KM. Mechanisms linking obesity to insulin resistance and type 2 diabetes. Nature 2006;444:840–846.
2 Van Gaal LF, Mertens IL, De Block CE. Mechanisms linking obesity with cardiovascular disease. Nature 2006;444:875–880.
3 Rosen ED, MacDougald OA. Adipocyte differentiation from the inside out. Nat Rev Mol Cell Biol 2006;7:885–896.
4 Rodeheffer MS, Birsoy K, Friedman JM. Identification of white adipocyte progenitor cells in vivo. Cell 2008;135:240–249.
5 Spalding KL, Arner E, Westermark PO et al. Dynamics of fat cell turnover in humans. Nature 2008;453:783–787.
6 Rodriguez AM, Elabd C, Delteil F et al. Adipocyte differentiation of multipotent cells established from human adipose tissue. Biochem Biophys Res Commun 2004;315:255–263.
7 Bezaire V, Mairal A, Ribet C et al. Contribution of adipose triglyceride lipase and hormone-sensitive lipase to lipolysis in hMADS adipocytes. J Biol Chem 2009;284:18282–18291.
8 Poitou C, Divoux A, Faty A et al. Role of serum amyloid a in adipocyte-macrophage cross talk and adipocyte cholesterol efflux. J Clin Endocrinol Metab 2009;94:1810–1817.
9 Zaragosi LE, Ailhaud G, Dani C. Autocrine fibroblast growth factor 2 signaling is critical for self-renewal of human multipotent adipose-derived stem cells. Stem Cells 2006;24:2412–2419.
10 Rodriguez AM, Pisani D, Dechesne CA et al. Transplantation of a multipotent cell population from human adipose tissue induces dystrophin expression in the immunocompetent mdx mouse. J Exp Med 2005;201:1397–1405.
11 Green H, Kehinde O. An established preadipose cell line and its differentiation in culture. II. Factors affecting the adipose conversion. Cell 1975;5:19–27.
12 Green H, Kehinde O. Spontaneous heritable changes leading to increased adipose conversion in 3T3 cells. Cell 1976;7:105–113.
13 Negrel R, Grimaldi P, Ailhaud G. Establishment of preadipocyte clonal line from epididymal fat pad of ob/ob mouse that responds to insulin and to lipolytic hormones. Proc Natl Acad Sci USA 1978;75:6054–6058.
14 Billon N, Monteiro MC, Dani C. Developmental origin of adipocytes: New insights into a pending question. Biol Cell 2008;100:563–575.
15 Tang W, Zeve D, Suh JM et al. White fat progenitor cells reside in the adipose vasculature. Science 2008;322:583–586.
16 Miranville A, Heeschen C, Sengenes C et al. Improvement of postnatal neovascularization by human adipose tissue-derived stem cells. Circulation 2004;110:349–355.
17 Sengenes C, Lolmede K, Zakaroff-Girard A et al. Preadipocytes in the human subcutaneous adipose tissue display distinct features from the adult mesenchymal and hematopoietic stem cells. J Cell Physiol 2005;205:114–122.
18 Zannettino AC, Paton S, Kortesidis A et al. Human mulipotential mesenchymal/stromal stem cells are derived from a discrete subpopulation of STRO-1bright/CD34/CD45(−)/glycophorin-A-bone marrow cells. Haematologica 2007;92:1707–1708.
19 Zimmerlin L, Donnenberg VS, Pfeifer ME et al. Stromal vascular progenitors in adult human adipose tissue. Cytometry A 2010;77:22–30.
20 Traktuev DO, Merfeld-Clauss S, Li J et al. A population of multipotent CD34-positive adipose stromal cells share pericyte and mesenchymal surface markers, reside in a periendothelial location, and stabilize endothelial networks. Circ Res 2008;102:77–85.
21 Amos PJ, Shang H, Bailey AM et al. IFATS collection: The role of human adipose-derived stromal cells in inflammatory microvascular remodeling and evidence of a perivascular phenotype. Stem Cells 2008;26:2682–2690.
22 Crisan M, Yap S, Casteilla L et al. A perivascular origin for mesenchymal stem cells in multiple human organs. Cell Stem Cell 2008;3:301–313.
23 Billon N, Iannarelli P, Monteiro MC et al. The generation of adipocytes by the neural crest. Development 2007;134:2283–2292.
24 Takashima Y, Era T, Nakao K et al. Neuroepithelial cells supply an initial transient wave of MSC differentiation. Cell 2007;129:1377–1388.
25 Keller GM. In vitro differentiation of embryonic stem cells. Curr Opin Cell Biol 1995;7:862–869.
26 Doetschman TC, Eistetter H, Katz M et al. The in vitro development of blastocyst-derived embryonic stem cell lines: Formation of visceral yolk sac, blood islands and myocardium. J Embryol Exp Morphol 1985;87:27–45.
27 Dani C, Smith AG, Dessolin S et al. Differentiation of embryonic stem cells into adipocytes in vitro. J Cell Sci 1997;110(pt 11):1279–1285.
28 Monteiro MC, Wdziekonski B, Villageois P et al. Commitment of mouse embryonic stem cells to the adipocyte lineage requires retinoic acid receptor beta and active GSK3. Stem Cells Dev 2009;18:457–463.

29 Billon N, Kolde R, Reimand J et al. Comprehensive transcriptome analysis of mouse embryonic stem cell adipogenesis unravels new processes of adipocyte development. Genome Biol 2010;11:R80.
30 Manley NR, Selleri L, Brendolan A et al. Abnormalities of caudal pharyngeal pouch development in Pbx1 knockout mice mimic loss of Hox3 paralogs. Dev Biol 2004;276:301–312.
31 DiMartino JF, Selleri L, Traver D et al. The Hox cofactor and proto-oncogene Pbx1 is required for maintenance of definitive hematopoiesis in the fetal liver. Blood 2001;98:618–626.
32 Selleri L, Depew MJ, Jacobs Y et al. Requirement for Pbx1 in skeletal patterning and programming chondrocyte proliferation and differentiation. Development 2001;128:3543–3557.
33 Kim SK, Selleri L, Lee JS et al. Pbx1 inactivation disrupts pancreas development and in Ipf1-deficient mice promotes diabetes mellitus. Nat Genet 2002;30:430–435.
34 Laurent A, Bihan R, Omilli F et al. PBX proteins: Much more than Hox cofactors. Int J Dev Biol 2008;52:9–20.
35 Slavin BG. Fine structural studies on white adipocyte differentiation. Anat Rec 1979;195:63–72.
36 Mountford P, Zevnik B, Duwel A et al. Dicistronic targeting constructs: Reporters and modifiers of mammalian gene expression. Proc Natl Acad Sci USA 1994;91:4303–4307.
37 Wdziekonski B, Villageois P, Dani C. Development of adipocytes from differentiated ES cells. Methods Enzymol 2003;365:268–277.
38 Wdziekonski B, Villageois P, Dani C. Differentiation of mouse embryonic stem cells and of human adult stem cells into adipocytes. Curr Protoc Cell Biol 2007;Chapter 23:Unit 23 24.
39 Elabd C, Basillais A, Beaupied H et al. Oxytocin controls differentiation of human mesenchymal stem cells and reverses osteoporosis. Stem Cells 2008;26:2399–2407.
40 Schnabel CA, Selleri L, Jacobs Y et al. Expression of Pbx1b during mammalian organogenesis. Mech Dev 2001;100:131–135.
41 Sanyal M, Tung JW, Karsunky H et al. B-cell development fails in the absence of the Pbx1 proto-oncogene. Blood 2007;109:4191–4199.
42 Otto TC, Lane MD. Adipose development: From stem cell to adipocyte. Crit Rev Biochem Mol Biol 2005;40:229–242.
43 Jurgens AS, Kolanczyk M, Moebest DC et al. PBX1 is dispensable for neural commitment of RA-treated murine ES cells. In Vitro Cell Dev Biol Anim 2009;45:252–263.
44 Brendolan A, Ferretti E, Salsi V et al. A Pbx1-dependent genetic and transcriptional network regulates spleen ontogeny. Development 2005;132:3113–3126.
45 Maumus M, Sengenes C, Decaunes P et al. Evidence of in situ proliferation of adult adipose tissue-derived progenitor cells: Influence of fat mass microenvironment and growth. J Clin Endocrinol Metab 2008;93:4098–4106.
46 Ban JY, Kang SA, Jung KH et al. The association of PBX1 polymorphisms with overweight/obesity and metabolic alterations in the Korean population. Nutr Res Pract 2008;2:289–294.
47 Zvonic S, Ptitsyn AA, Conrad SA et al. Characterization of peripheral circadian clocks in adipose tissues. Diabetes 2006;55:962–970.


See www.StemCells.com for supporting information available online.

Monteiro et al. Supplemental file 1 (methods)

WAT isolation and fractionation

Periepididymal WAT was obtained from ten weeks-old C57Bl/6J male mice in accordance with the European regulations for the care of research animals. Human subcutaneous adipose tissue samples were obtained from Caucasian women undergoing plastic surgery. Subjects included 35 women (mean BMI ± SEM = 29.6 ± 1.1 kg/m2, range 18.4-42.5; mean age ± SEM = 40.7 ± 2.01 years, range 24–71 years). Fat collection protocols were approved by the Institutional Research Board of Inserm and the Toulouse/Nice University Hospital Ethics Committee. Adipocyte fraction (AF) and SVF were obtained by collagenase digestion as previously described [24]. Native $CD34^+/CD31^+$ cells (endothelial cells) [34], $CD34^+/CD31^-$ (APs) [16, 17], $CD34^-/CD14^+/CD31^+$ (macrophages) [35, 36] and $CD34^-/CD14^-/CD3^+$ (lymphocytes) [37] were isolated by immunoselection/depletion method as previously described [38]. hMADS cells were obtained from the stroma of human adipose tissue isolated from infant donors, as described previously [6, 34].

siRNA transfection of hMADS cells

HMADS cells were transfected by *PBX1* siRNA duplexes using HiPerfect reagent. One day before small interfering RNA (siRNA) transfection, proliferating hMADS cells were plated in transfection medium (TM) containing 2% FCS and 2.5 ng/ml FGF2 at either 7400 cells/cm2 or 37000 cells/cm2, to investigate their effects on cell proliferation or adipocyte differentiation, respectively. TM was composed of DMEM low glucose/ MCDB (60%/40%) supplemented with 100µM ascorbic acid sodium salt, 10 nM Dex, 10 µg/mL insulin, 5 µg/mL transferring and 50 ng/mL selenium (ITS mix). HMADS cells were transfected in 0.5% serum TM with 30 nM (siRNA) duplexes using the HiPerfect reagent (Qiagen, Courtaboeuf,

France), according to the manufacturer's instructions. For proliferation assays, 2.5 ng/mL FGF2 wad added. We used a control siRNA duplex with no human target mRNA (Eurogentec, Angers, France), or 2 siRNA duplexes against *PBX1,* comprising the target sequence 5'ggaagcaggacauuggaga3' (siRNA pbx1 #1) or 5'ccaauauuuaugcugccaa3' (siRNA pbx1 #2). HiPerfect-siRNA mixtures were replaced by PM one day after transfection for proliferation assays, or by DM 2 days after transfection (designated as day 0) for adipocyte differentiation assays.

Cell cycle analysis

Cell cycle distribution was evaluated using a cyclin A/ propidium iodide (PI) double labelling. hMADS cells were synchronised before cell cycle assays were performed. Briefly, cells were plated on 100 mm^2 dishes (4,500 cells/cm^2) and grown in TM containing 0,5% FCS and 2.5 ng/ml FGF2. After 1 day, cells were transfected with siRNAs as described above and left for 48H in the absence of serum and FGF2. Cells were then incubated for 24H in TM containing 0,5% serum and 2.5 ng/m FGF2. For cell cycle analysis, cells were trypsined, fixed in cold 70% ethanol and permeabilised in a PBS / 1% triton (v/v) solution for 10 minutes. Cell cycle distribution was evaluated using cyclin A/ propidium iodide (PI) double labelling. Cells were incubated with an anti-cyclin A antibody (Novocastra, Rungis, France) for 1H, followed by incubation with an Alexa Fluor 488 conjugated goat anti-mouse antibody (Invitrogen, Cergy Pontoise, France) for 30 minutes. Cells were then resuspended in 500µl PBS containing NP40 (0,1%), RNase A (20µg/ml) and propidium iodide (40µg/ml). Staining acquisition was performed on a FACSCALIBURE ™ on at least 10,000 events per sample and analysed using the CellQuest ™ software (BD, Pont de Claix, France). Cyclin A is expressed at the end of the G1 phase/beginning of the S phase through the end of the G2 phase, while PI reflects the DNA content of the cells. Thus, cells in the G0/G1 phase display a

1N DNA content (low PI) and no cyclin A expression (Fig.4C, a, R2 gate), while cells in the S/G2 phases show a 4N DNA content (high PI) and high cyclin A expression (R3 gate), and cells in the M phase have a 4N DNA content (high PI) and low cyclin A expression (R4 gate).

RNA isolation and Quantitative real-time-PCR (qPCR)

Total RNA was extracted using the Rneasy kit (Qiagen, Courtaboeuf, France) and RT-PCR analysis was conducted as described previously [18]. All primers sequences are detailed in Sup.File 4. For qPCR, final reaction volume was 25 µl, including specific primers (0.4 µM), 10 ng of reverse transcribed RNA and 12.5 µl SYBR green master mix (Eurogentec, Angers, France). qPCR conditions were as follows: 2 min at 50°C, 10 min at 95°C, followed by 40 cycles of 15 sec at 95°C, 1 min at 60°C. Real-time PCR assays were run on ABI Prism GeneAmp 7500 or 7700 real-time PCR machines (PerkinElmer Life Sciences, Courtaboeuf, France). Relative gene expression was calculated by the dCT method and normalized to the geometric mean of the expression of three reference genes, unless otherwise indicated. The mouse reference genes were *βactin*, *Gapdh* and *Tbp*, and the human reference genes were *G6PDH*, *POLR2A*, and *TBP*, or *18s*.

List of primers used for qPCR

gene	RNA Accession N°	forward primer (5'-3')	reverse primer (5'-3')
a) Mouse primers			
Adiponec	NM_00479	gcaggcatcccaggacat	gcccttcagctcctgtcattc
β-actin	NM_00739	ctgtgctatgttgccctggat	gctcattgccgatggtgatc
Fabp4	NM_02440	cttcaaactgggcgtggaa	ctagggttatgatgctcttcac
Gapdh	NM_00808	catggccttccgtgttccta	tgcctgcttcaccaccttct
Leptin	NM_00849	acctgctccgggtacatgtt	cttcacggtgctcccaaaga
Lpl	NM_00850	gaggccagggtccaggttt	gccaggcaggaagcagag
Pbx1	NM_00878	ggcggaagagacggaat	tgccgcacttcttggctaac

Pbx1a	NM_00878	agccaacgtgcaatcaca	gatgccctgcggactgta
Pbx1b	NM_18335	tgccaaaacggctgtcac	ggtatccacccgctgagttg
Polr2a	NM_00908	tcgaattgacttgcgtttcca	gcaaagttggctgacgattga
Pparγ2	NM_01114	acagcaaatctctgttttatg	gcttgatctcaaaggaatgcg
Sox1	NM_00923	gccgagtggaaggtcatgt	tgtaatccgggtgttccttcat
Sox10	XM_128139	cacatcgacttcggcaac	ccgttgggtggcaggtatt
Tbp	NM_01368	gtgcacaggagccaaga	cacagctccccaccatgttc
b) Human primers			
G6PDH	NM_00428	accttcgcagccgtcctagt	atccgagcgtagcccactct
CEBPα	NM_00436	aaccaaccgcacatgca	ggcagagggagaagcaga
CEBPβ	NM_00519	aaccaaccgcacatgca	ggcagagggagaagcaga
FABP4	NM_00144	tgtgcagaaatgggatgg	caacgtcccttggcttatgct
LPL	NM_00023	tggaggtacttttcagccag	tcgtgggagcacttcactagc
PBX1AB	NM_00258	ggcggaagagacggaat	tgccgcgcttcttggctaac
		Hs00231228, Applied Biosystems (Assays on	
POLR2A	NM_00093	tgggtgtgccccgacttaa	tccagacggcacagaatatc
PPARγ	NM_13871	agcctcatgaagagccttc	tccggaagaaacccttgca

Western blot analysis

Whole cell extracts, SDS-polyacrylamide gel electrophoresis, blotting, and enhanced chemiluminescence were performed as described previously [9]. Primary antibodies were mouse monoclonal antibodies against either PBX1a or PBX1b [40] (dilution 1:1000). Secondary horseradish peroxidase-conjugated antibody was purchased from Promega (Charbonnières-les-Bains, France).

A

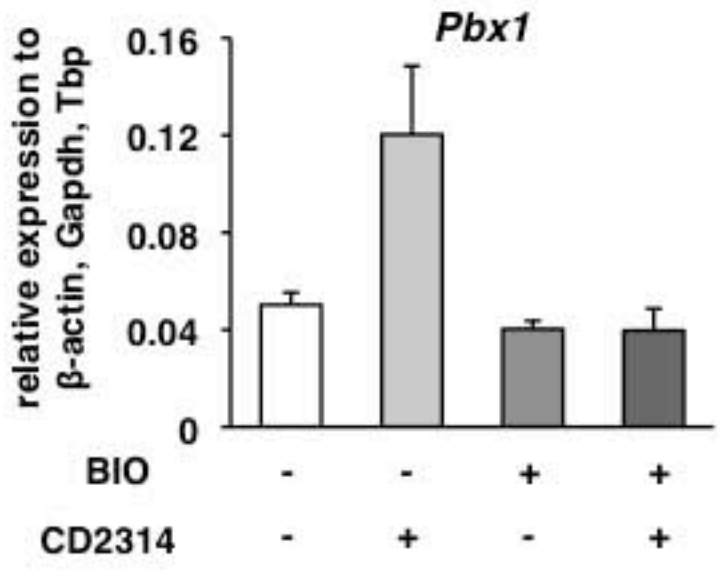
Pbx1
relative expression to β-actin, Gapdh, Tbp
0.16
0.12
0.08
0.04
0
BIO - - + +
CD2314 - + - +

B

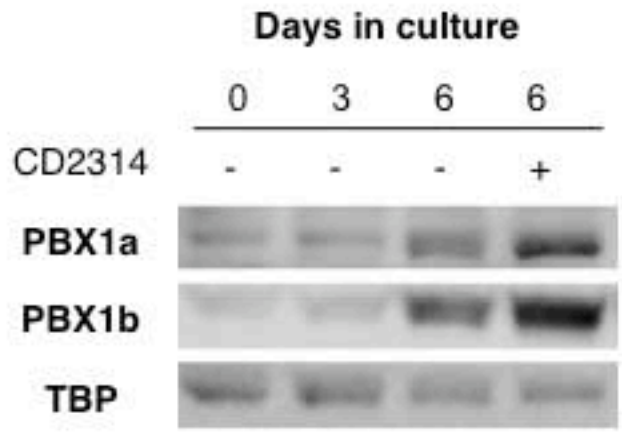
Days in culture
0 3 6 6
CD2314 - - - +
PBX1a
PBX1b
TBP

Monteiro et al. Sup File 3

Proliferating cells

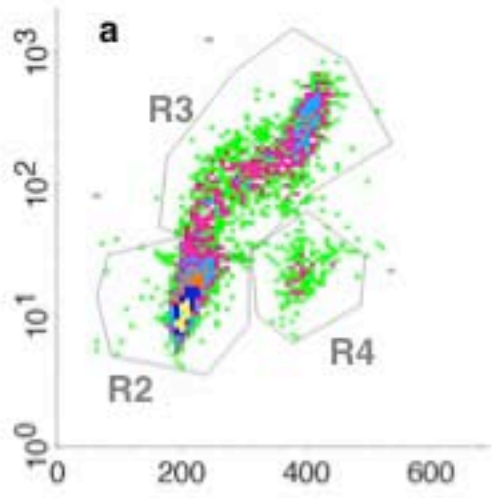

No FCS 48H

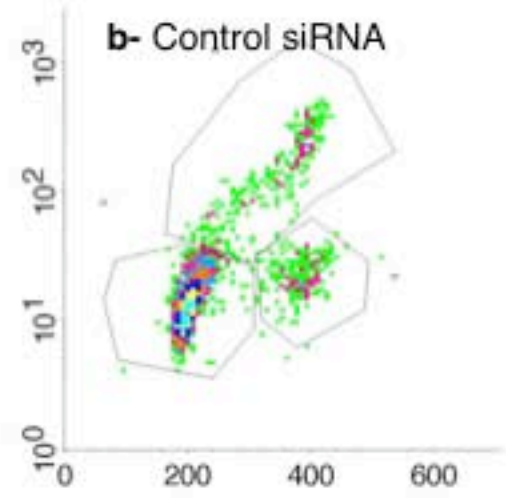

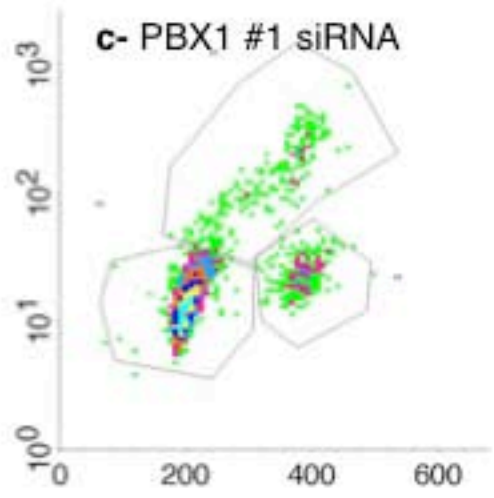

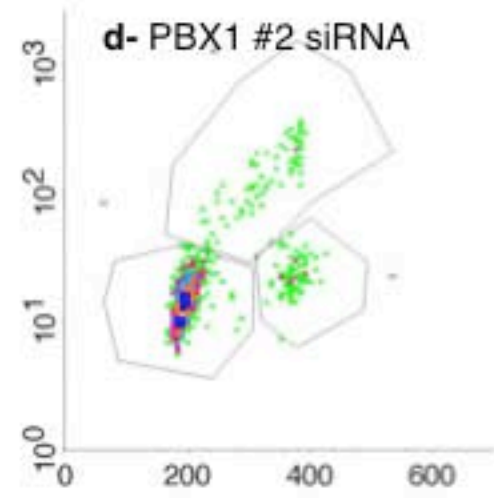

Restimulation FCS 24h

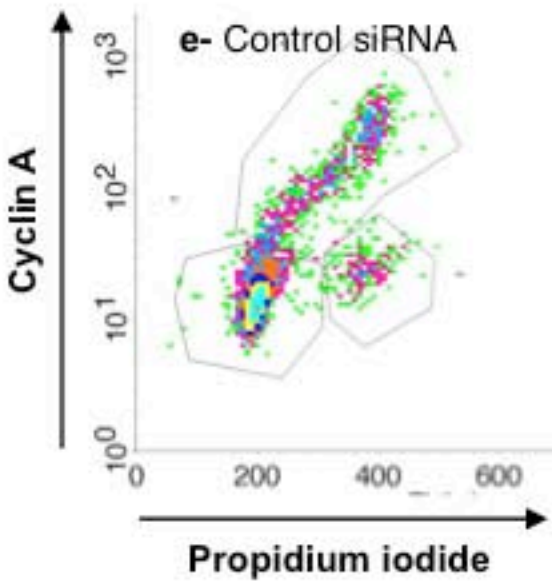

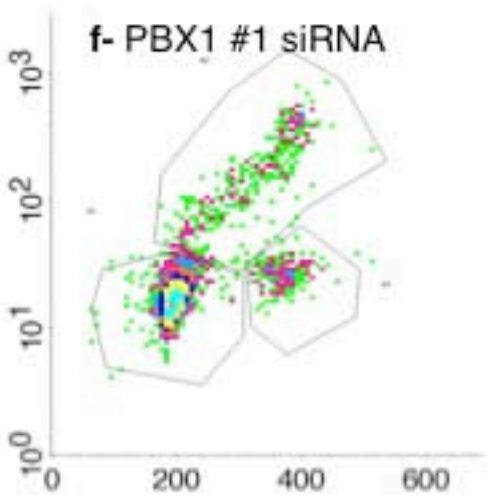

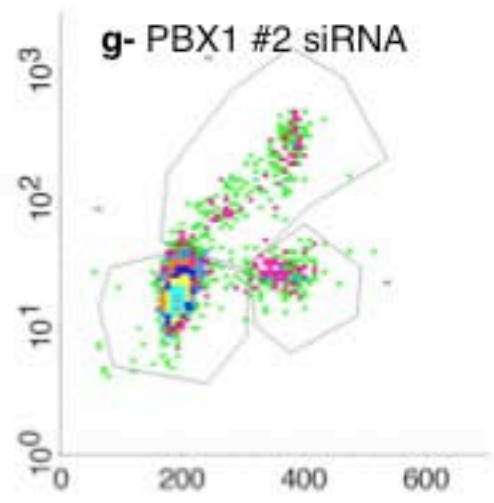

A

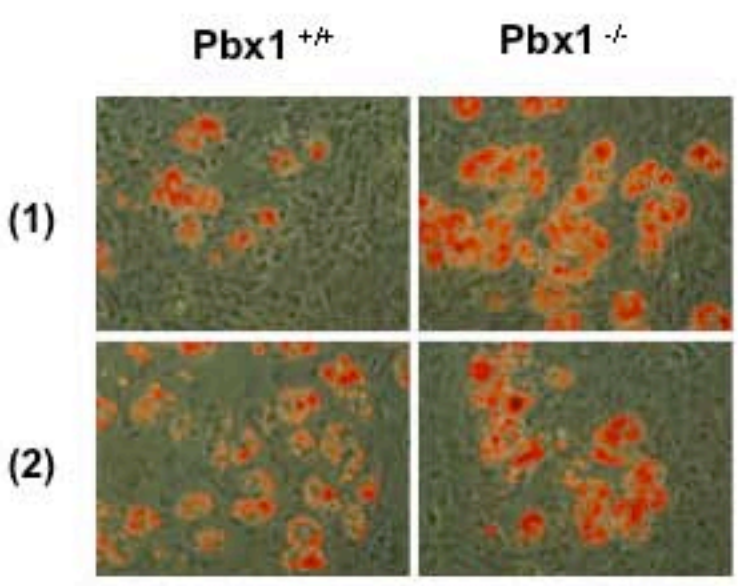
Pbx1 +/+
Pbx1 -/-
(1)
(2)

B

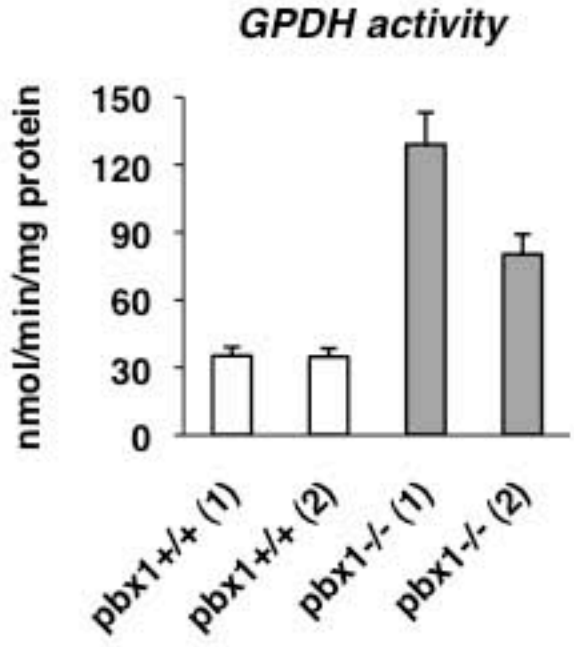
GPDH activity
nmol/min/mg protein
150
120
90
60
30
0
pbx1+/+ (1)
pbx1+/+ (2)
pbx1-/- (1)
pbx1-/- (2)

C

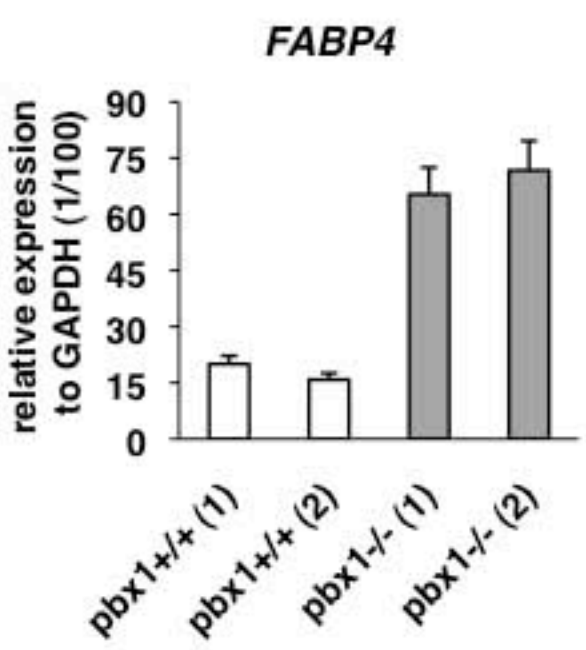
FABP4
relative expression to GAPDH (1/100)
90
75
60
45
30
15
0
pbx1+/+ (1)
pbx1+/+ (2)
pbx1-/- (1)
pbx1-/- (2)

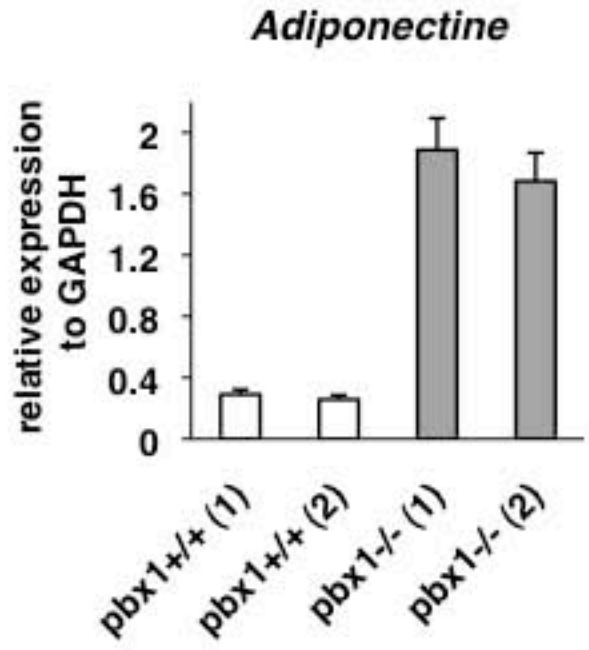
Adiponectine
relative expression to GAPDH
2
1.6
1.2
0.8
0.4
0
pbx1+/+ (1)
pbx1+/+ (2)
pbx1-/- (1)
pbx1-/- (2)